Monte Carlo computation of the effective Sherman function

M Drągowski[1], M Włodarczyk[1], J Ciborowski[1], G Weber[2], J Enders[3], Y Fritzsche[3] and A Poliszczuk[1]

[1] University of Warsaw, Faculty of Physics, Pasteura 5, 02093 Warsaw, Poland
[2] Helmholtz Institut Jena, Fröbelstieg 3, 07743 Jena, Germany
[3] Technische Universität Darmstadt, Institut für Kernphysik, Schlossgartenstraße 9, 64289 Darmstadt, Germany

E-mail: mdragowski@fuw.edu.pl

Abstract. The PEBSI Monte Carlo code was recently upgraded towards usefulness to compute the effective Sherman function, which is used in electron Mott polarimetry. The results of the simulation were compared to experimental data for a 100 keV polarized electron beam. The properties of the effective Sherman function, as well as the problem of experiment optimization were analyzed using the data from the simulation.

1. Introduction

The method of Mott polarimetry is used to determine the spin–polarization of electron beams, taking advantage of the dependence of Mott scattering cross section on spin direction due to the spin–orbit interaction. It is used in a wide range of electron energies (from keV up to several MeV), both in basic research, as well as numerous applications (e.g., spin–polarized scanning electron microscopy and spin–resolved photoemission spectroscopy).

The method is based on measuring the azimuthal asymmetry[1] in Mott scattering of a polarized electron beam on thin targets made of heavy elements (e.g., Au). The degree of the observed asymmetry is related to the Sherman function, dependent on scattering angle and beam energy.

However, the pure Sherman function, which may be calculated theoretically, corresponds to scattering on a single atom. On the other hand, the measurement is performed on targets of finite thicknesses. In this case the effective Sherman function has to be used, in which multiple interactions of the electron with several target atoms are accounted for. These effects cannot be calculated analytically and simulation tools must be used for modeling the passage of polarized electrons through matter. Other background processes changing the polarization state of the electrons also take place (in particular Møller scattering and bremsstrahlung emission), leading to the decrease of the analyzing power of the polarimeter.

Furthermore, experimental data covering a wide range of scattering angles exist for a few energies only[2]. Therefore, simulation seems to be a natural choice for a systematic study of the

[1] i.e., with detectors placed symmetrically about the beam axis at a given angle with respect to the beam direction
[2] the construction of a typical Mott polarimeter does not allow for convenient change of the angle

properties of the Sherman function (especially in energy ranges where few or no experimental data exist) and is beneficial because of the fact that it allows to investigate additional effects besides the value of Sherman function and angular distribution of scattered electrons (e.g., sources of background, optimal detector cuts etc.).

The angular and energy distributions of scattered electrons were studied, both for all particles and based on interaction types which took place in the target. Electrons originating from Møller scattering were found to have important impact on the effective Sherman function if low energy particles are taken into account, thus leading to significant decrease of the analyzing power of the polarimeter. Furthermore, simple dependence on target thickness is not observed anymore in this case. This effect can be avoided by imposing proper detector cuts on electron energy.

Optimizing the measurement comes down to choosing the optimal scattering angle and target thickness for electrons of a given energy. Therefore, the angular dependence of the Sherman function was analyzed from this perspective. Simulation allows to exclude regions less suitable for measurement (e.g., where the Sherman function undergoes rapid changes with scattering angle[3]). The dependence of the Sherman function on target thickness (for a given scattering angle) was also analyzed and compared to commonly used parametrizations.

2. Interactions of electrons with matter

2.1. Mott scattering

The cross section for Mott scattering (i.e., the elastic scattering of electrons on atomic nuclei) depends on electron polarization according to the following relation [1]:

$$\frac{\mathrm{d}\sigma_{\mathrm{Mott}}}{\mathrm{d}\Omega} = \left(\frac{\mathrm{d}\sigma_{\mathrm{Mott}}}{\mathrm{d}\Omega}\right)_0 (1 + S(\theta)\vec{P}\cdot\vec{n}),$$

where $(\mathrm{d}\sigma_{\mathrm{Mott}}/\mathrm{d}\Omega)_0$ is the cross section corresponding to scattering of unpolarized electrons, $S(\theta)$ is the Sherman function, θ is the scattering angle, $\vec{P}$ is the polarization vector of the incident electron and $\vec{n}$ is the unit vector normal to the scattering plane.

The Mott scattering cross section is calculated from the Dirac equation, taking into account the spin–orbit interaction (contrary to the Rutherford cross section which neglects this effect). The numerical values depend on the atomic potential assumed in the calculations; at low energies and low scattering angles the screening of the nuclear Coulomb potential by the electron cloud cannot be neglected (as in the Rutherford formula assuming pure Coulomb field of the nucleus).

Experiments are carried out using detectors placed symmetrically about the beam axis at a given angle θ with respect to the beam direction. The measurement is typically performed in backscattering, as the largest effect (S) is obtained for large scattering angles. The quantity of interest is the azimuthal (left–right) asymmetry in the number of electrons detected in the two detectors, A_{LR}, which allows to calculate the polarization of the electron beam according to the following formula:

$$\vec{P}\vec{n} = \frac{A_{LR}}{S}.$$

In practice the theoretical value of S is replaced with its effective value S_{eff} in the above equation. It is worth stressing that this method is sensitive only to the spin projection on the direction perpendicular to the scattering plane.

Both the unpolarized cross section and the Sherman function are defined by two scattering amplitudes, $f(\theta)$ – spin–conserving amplitude and $g(\theta)$ – spin–flip amplitude, according to the following equations [2]:

$$\left(\frac{\mathrm{d}\sigma_{\mathrm{Mott}}}{\mathrm{d}\Omega}\right)_0 = |f(\theta)|^2 + |g(\theta)|^2,$$

[3] this could not be taken into account in experiments in which the Sherman function was determined by a single measurement

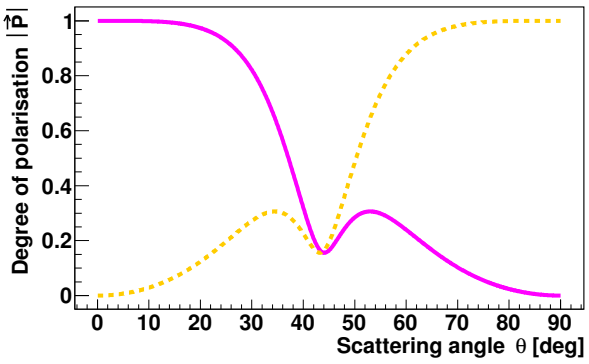

Figure 1. Transfer of polarization from a 100 keV, 100% polarized beam electron to the secondary Møller electrons; dependence of the length of the polarization vector on the scattering angle θ for two electrons in the final state (θ is measured for the electron whose polarization is plotted with the solid line).

$$S(\theta) = i\frac{fg^* - f^*g}{|f(\theta)|^2 + |g(\theta)|^2}.$$

Furthermore, the polarization vector of the electron after the scattering, $\vec{P}'$, is expressed by the initial polarization, $\vec{P}$, Sherman function $S(\theta)$ and two additional functions, $T(\theta)$ and $U(\theta)$ [2]:

$$\vec{P}' = \frac{(\vec{P}\cdot\vec{n} + S(\theta))\vec{n} + T(\theta)\vec{n}\times(\vec{n}\times\vec{P}) + U(\theta)(\vec{n}\times\vec{P})}{1 + S(\theta)\vec{P}\cdot\vec{n}},$$

which are also defined by the scattering amplitudes:

$$T(\theta) = \frac{|f(\theta)|^2 - |g(\theta)|^2}{|f(\theta)|^2 + |g(\theta)|^2},$$

$$U(\theta) = \frac{fg^* + f^*g}{|f(\theta)|^2 + |g(\theta)|^2}.$$

The S, T and U functions have the following interpretation: (i) S describes the change of the polarization vector component perpendicular to the scattering plane, (ii) T describes the change of the polarization vector component parallel to the scattering plane, and (iii) U describes the polarization appearing in the scattering plane, but perpendicular to the initial polarization vector.

2.2. Møller scattering

Møller scattering (i.e., the elastic scattering of two electrons) is the second most important process if the cross sections are considered. Its significance follows also from the fact, that it results in a relatively large change of both the momentum and the polarization of the interacting electron.

Interestingly, the final spin states of individual Møller electrons after the scattering are not unambiguously determined, as the particles may be entangled [3]. It is, however, possible to calculate the mean polarization vectors from the spin density matrix of the final state.

In a typical experimental case when the beam electron is highly polarized and the target electron is unpolarized, the two electrons in the final state share the initial polarization (i.e., they are only partly polarized). This effect is illustrated quantitatively in Fig. 1, in which the dependence of the degree of polarization (the length of the polarization vector) is shown for both electrons in the final state as a function of the scattering angle. It can be seen that in case of symmetric scattering both electrons have the same polarization (due to their indistinguishability), while in general one of the electrons inherits majority of the initial polarization. The electron with higher energy is always more polarized.

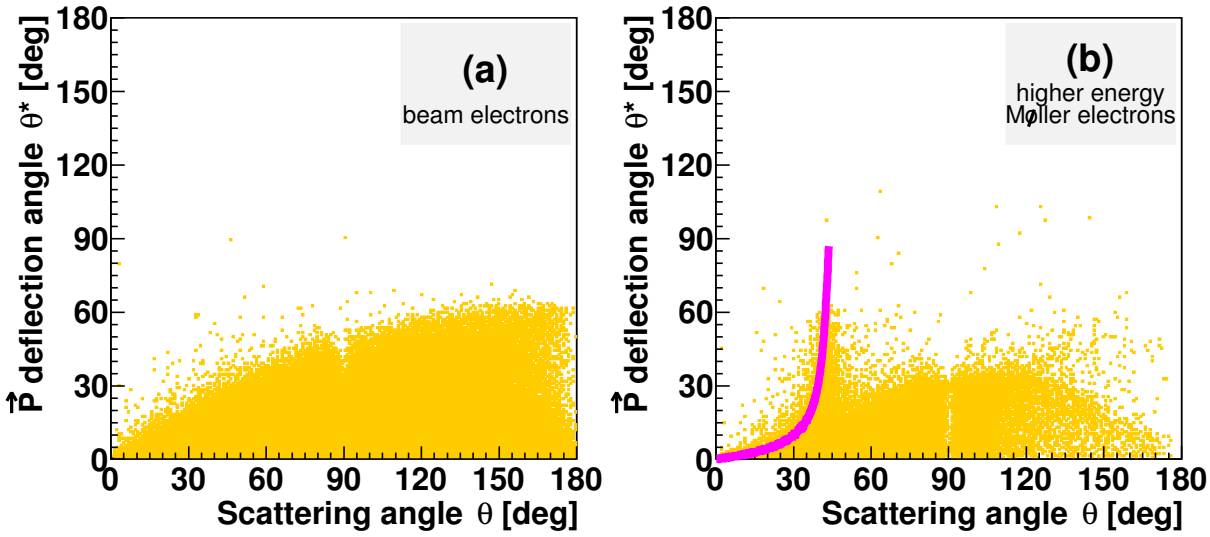

Figure 2. Distribution of simulated events as a function of the angles θ^* and θ (between the initial and final polarization and the initial and final momentum vectors, respectively) for a 10 nm target; (a) only Mott–scattered electrons (no energy cut), (b) higher energy Møller electrons (above 50 keV). The curve demonstrates the theoretical prediction for Møller electrons.

2.3. Implementation in PEBSI

The PEBSI Monte Carlo simulation was originally written to simulate bremsstrahlung accompanying passage of polarized electrons through thin target foils [4]. It was recently upgraded towards usefulness to compute the effective Sherman function. The description of Mott scattering was improved and polarization transfer in Møller scattering was included in the code.

The model of Mott scattering is based on the theoretical formalism presented above. However, calculation of the scattering amplitudes requires the use of numerical methods due to the mathematical complexity of the problem; the method was originally proposed by Sherman [5]. In the PEBSI package their values are calculated using the ELSEPA code, in which they are derived from the Dirac equation assuming the Thomas–Fermi–Dirac atomic potential [6].

In order to simulate Møller scattering, analytical formulae derived according to [3] are used both for the cross section and the polarization transfer. Møller scattering regards, however, scattering on (quasi) free electrons only. Therefore, in case when the binding energy of the target electron cannot be neglected compared to the kinetic energy (which is typically the case for electron shells other than the outermost one) a combination of the formula proposed by Bote et al. [7] and the MRBEB model by Guerra et al. [8] was used to simulate electron impact ionization.

Bremsstrahlung is the least significant process to be considered, as the emission of a bremsstrahlung photon is unlikely to significantly change the polarization state of the electron. Therefore, this effect was neglected in the present work.

3. Results

3.1. Depolarization

Accounting for the polarization change caused by Møller scattering in the PEBSI code allowed us to observe interesting effects related to this interaction. The dependence between the change of polarization and momentum directions is illustrated in the scatter plots in Fig. 2; θ^* denotes

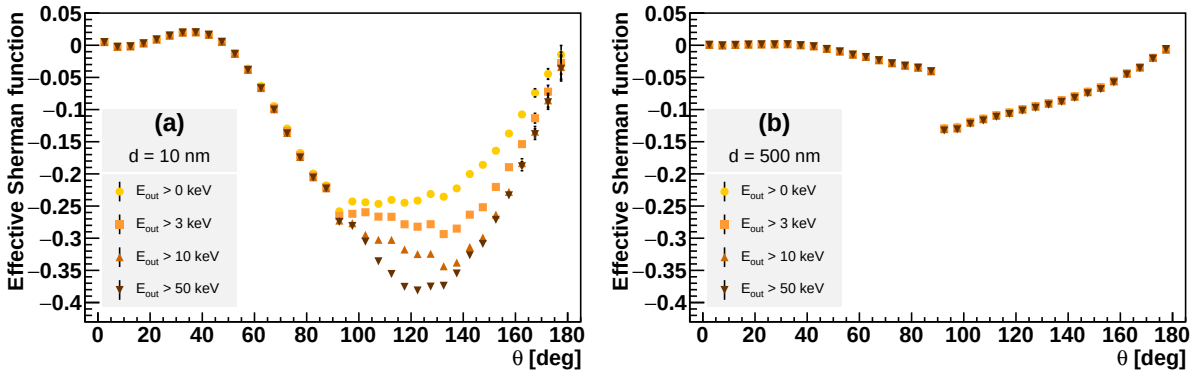

Figure 3. Simulated effective Sherman function; effect of the low energy cuts on electron energy for 100 keV electrons impinging on 10 and 500 nm Au targets.

the angle between the initial and final polarization vectors, θ – between the initial and final momentum vectors (which is equivalent to the scattering angle[4]). The plots were made separately for electrons that did not undergo Møller scattering and for more energetic Møller electrons (above 50 keV in case of 100 keV incident beam). It can be seen that these two classes of events differ from each other, as for Møller electrons one may expect greater change in the polarization direction, even in case of a small change in momentum direction. This result is in agreement with the theoretical model describing Møller scattering; the theoretical prediction was marked in the figure with a solid line.

3.2. Simulated effective Sherman function

The impact of Møller scattering on the effective Sherman function can be analyzed by computing its value with different low energy cuts on the energy of the electrons leaving the target (which corresponds to the detector cuts determining the energy of the electrons recorded in the experiment). The resulting dependences of the effective Sherman function on the scattering angle, plotted for several values of the energy cuts, are shown in Fig. 3 for two different target thicknesses (10 and 500 nm). It can be noticed that in case of the thin target the low energy electrons significantly affect the value of the effective Sherman function, leading to a large decrease of the analyzing power of the polarimeter. This effect decreases with increasing target thickness and is no longer observed in case of the thickest target. Nevertheless, this phenomenon is strictly related to Møller scattering, as by analyzing the energy distributions of the electrons leaving the target we found that electrons with that low values of energy always originate from this interaction.

The reliability of the simulation was proved by comparison with available experimental data for a 100 keV polarized electron beam incident on 10 — 500 nm Au targets, published by Kohashi et al. [9]. The result for a 500 nm target is shown in Fig. 4. In this case the cut on electron energy was chosen as 50 keV, which corresponds to the conditions of the experiment. The comparison was made in a wide scattering angle range (from 20 to 160 degrees) and the results were found in good agreement. Although there is a systematic difference, the agreement can be considered satisfactory given the simulation is based on a purely theoretical model, with no empirical corrections.

[4] here we refer to the effective scattering angle that may be observed in an experiment, as opposed to the theoretical scattering angle in a single scattering event

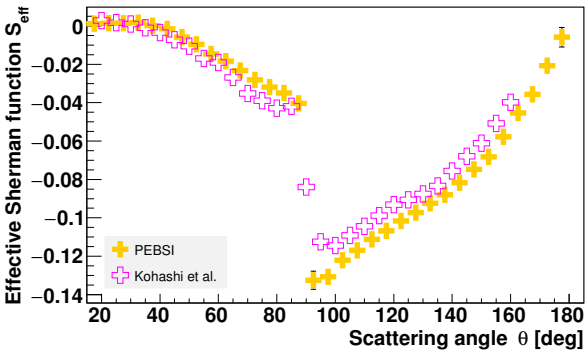

Figure 4. Simulated effective Sherman function; comparison with measurement for 100 keV electrons impinging on a 500 nm Au target.

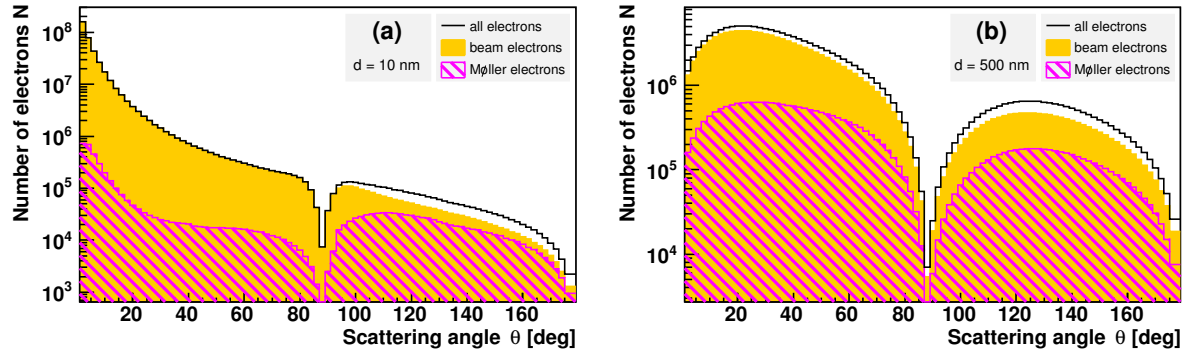

Figure 5. Scattering angle distribution for 100 keV electrons impinging on 10 and 500 nm Au targets.

3.3. Parametrizations

The scope of our study was not limited to the computation of the effective Sherman function for certain conditions. In particular, thanks to the possibility to generate an amount of data corresponding to different target thicknesses, we shortly addressed the problem of experiment optimization and extrapolation procedures for the Sherman function.

Optimal experimental conditions correspond to the maximum of the figure–of–merit, FoM, defined as [9, 10]:

$$\mathrm{FoM}(E,\theta,d) \propto S^2_{\mathrm{eff}}(E,\theta,d)\, N(E,\theta,d),$$

where $N(E,\theta,d)$ is the total number of electrons recorded in the detectors placed at a given angle θ. The form of this function is intended to balance the resolution of the measurement (which is proportional to S_{eff}) and the statistical uncertainty (which is proportional to $\sqrt{N}$). The optimal target thickness corresponds to the maximum of this function for a given energy and scattering angle.

The distribution of the scattering angle changes significantly with the target thickness, which results in a complicated $N(d)$ dependence. This is illustrated in Fig. 5 where the scattering angle distribution is shown for two different target thicknesses (10 and 500 nm). It can be seen that in case of thicker targets electrons are more likely to be scattered at large angles. However, the value of the effective Sherman function decreases with increasing target thickness which makes it necessary to take both effects into account.

The effective Sherman function is often parametrized in terms of target thickness in order to provide a functional form of the figure–of–merit and to interpolate the value of the effective Sherman function between the measured or simulated data points. There are two

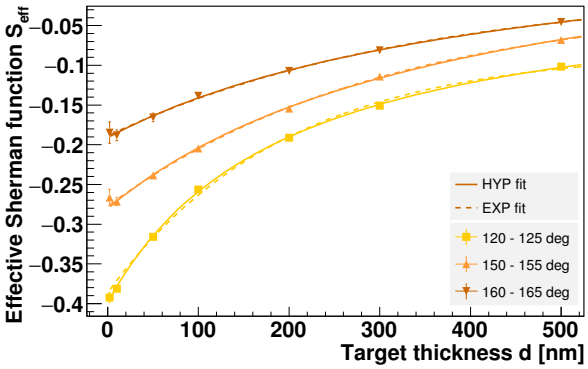

Figure 6. Simulated effective Sherman function; dependence on target thickness for 100 keV electrons impinging on 2 — 500 nm Au targets.

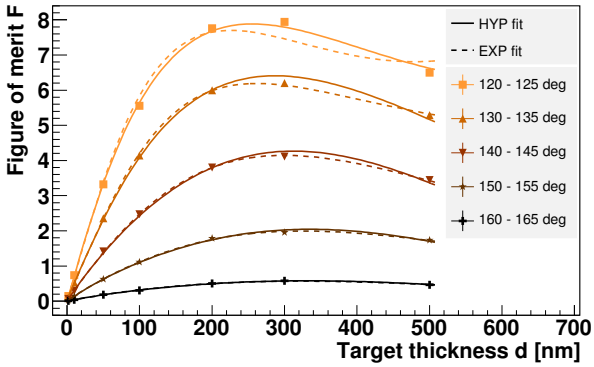

Figure 7. Figure–of–Merit FoM $= S_{eff}^2 N$ for 100 keV electrons impinging on 2 — 500 nm Au targets.

parametrizations commonly used in the literature [9, 10, 11]:

$$\text{hyperbolic: } S_{\text{eff}}^{\text{HYP}}(d) = S_c + \frac{S_0 - S_c}{1 + \alpha_H\, d},$$

$$\text{exponential: } S_{\text{eff}}^{\text{EXP}}(d) = S_c + (S_0 - S_c)\exp(-\alpha_E\, d).$$

The result of the comparison to the data from our simulation is shown in Fig. 6. It can be seen that both parametrizations describe the simulated data reasonably well. The difference between the two fits is more pronounced in case of lower scattering angles.

Having the results of the analyses of both the number of electrons scattered to the detectors and the dependence of the effective Sherman function on target thickness allowed us to calculate the figure–of–merit. The dependence of FoM on target thickness is shown in Fig. 7, for several values of the scattering angle. It can be noticed that in this case there is a significant difference between the two parametrizations of $S_{\text{eff}}(d)$; one of the two functions is found more appropriate depending on the scattering angle. Nevertheless, applying the procedure described above to the simulated data allows one to determine the optimal target thickness for Mott polarimetry measurements, which is of high practical significance.

4. Summary

The values of the simulated effective Sherman function were compared to the experimental data for 100 keV electrons and the results of these first comparisons were found highly encouraging. Further analyses of the behavior of the Sherman function and of the general properties of studied phenomena revealed many interesting effects that did not get enough attention in the past.

These first results suggest many prospective applications for our code, including, but not limited to: (*i*) computation of the effective Sherman function, (*ii*) experiment optimization, (*iii*) depolarization of electron beams passing through matter. Firstly, PEBSI allows to compute the Sherman function for arbitrary experimental conditions (i.e., also when no experimental data exist). Secondly, a comprehensive analysis and optimization of an experiment requires collecting a large amount of data, which may be difficult to perform by a direct measurement. Thirdly, its applications are definitely not limited to the computation of the effective Sherman function only. The PEBSI code allows to investigate any effect related to the change of the polarization state of an electron beam passing through matter. Such studies may be essential for many other

applications, which require the precise knowledge of the polarization of an electron taking part in an interaction.

In order to prove the applicability of our simulation in other energy ranges in which Mott polarimetry is used it would be necessary to compare to other experimental data, especially for higher energies. This computation is, however, time consuming due to the low cross sections for studied processes. Nevertheless, further validation is currently ongoing.

Acknowledgments

We thank Prof. J. Rembieliński and Prof. P. Caban for discussions regarding polarization effects in Møller scattering; Prof. A. Jabłoński for consultations regarding the ELSEPA package. This work was supported from the funds of the National Science Centre: (1) as a part of the research project, contract/decision DEC-2012/06/M/ST2/00430; (2) as a postdoc project (M.W.) contract/decision DEC-2013/08/S/ST2/00551.

References

[1] Mott N F 1929 *Proc. R. Soc.* A **124** 425
[2] Kessler J 1985 *Polarized Electrons* 2nd ed. (Berlin: Springer)
[3] Caban P, Rembieliński J and Włodarczyk M 2013 *Phys. Rev.* A **88** 032116
[4] Weber G et al. 2012 *Nucl. Instr. Meth. Phys. Res.* B **279** 155
[5] Sherman N 1956 *Phys. Rev.* **103** 1601
[6] Salvat F, Jablonski A and Powell C J 2005 *Comput. Phys. Commun.* **165** 157
[7] Bote D, Salvat F, Jablonski A and Powell C J 2009 *Atomic Data and Nuclear Data Tables* **95** 871
[8] Guerra M, Amaro P, Machado J and Santos J P 2015 *J. Phys.* B **48** 18
[9] Kohashi T, Konoto M and Koike K 2006 *Jpn. J. Appl. Phys.* **45** 6468
[10] Gay T J and Dunning F B 1992 *Rev. Sci. Instrum.* **63** 1635
[11] Gay T J et al. 1992 *Rev. Sci. Instrum.* **63** 114